Design of a directive source using the radiation mode method and a sound zone algorithm

Manuel MELON[(1)], Maryna SANALATII[(2)], Philippe HERZOG[(3)], Régine GUILLERMIN[(4)], Nicolas POULAIN[(2)] & Jean Christophe LE ROUX[(2)]

[(1)]LAUM UMR CNRS 6613, Av. Olivier Messiaen, 72085 Le Mans Cedex 9, France, manuel.melon@univ-lemans.fr

[(2)]Centre de Transfert de Technologie du Mans (CTTM), 20 rue Thalès de Milet, 72000 Le Mans, France

[(3)]ARTEAC-LAB SAS, Place de l'Innovation, 8 allées Léon Gambetta, 13001 Marseille, France

[(4)]Laboratoire de Mécanique et d'Acoustique (LMA), UMR CNRS 7031, 4 impasse Nikola Tesla, 13000 Marseille, France

Abstract

A common mean to achieve narrow directive patterns consists in using loudspeaker arrays. Generally, the position of the sources in the array is arbitrarily fixed, for instance by using a regular spacing. The filters for each speaker are then calculated to get the desired acoustic field. In some cases, the predefined speaker positions might not be the optimal ones. Moreover, the diffraction on the source body may not be negligible for medium range applications. In this paper, we propose a two-step approach to overcome these problems. First, the radiation modes of the enclosure are computed. They are used in an inverse scheme, to find the most efficient vibration patterns over the enclosure, able to generate a target field at some chosen frequencies. These vibration patterns are then used to define the positions and sizes of actual loudspeakers on the enclosure. In a second step, a sound zone algorithm is used to calculate the signals driving the speakers. This yields a very narrow directivity pattern with reduced side lobe amplitudes. The proposed method is tested both numerically and experimentally and results are reported. A discussion about the pros and cons of the proposed approach is then provided.

Keywords: Sound, Insulation, Transmission

1 INTRODUCTION

The problem of acoustical sound zoning (SZ) is widely studied in the literature. Generally, the SZ techniques use arrays of loudspeakers which are intuitively placed, what is not always an optimal choice [9, 25, 7, 26, 5]. The problem of sources position optimisation has also been addressed in the literature. Two main strategies were proposed: (1) selection of the most suitable positions among proposed ones [3, 17, 15] or (2) optimisation of the positions [13, 4, 1, 2, 8, 24] via minimisation of a cost function or by using the gradient method. In this work we propose to design the source through the radiation mode (RM) method [23], which allows to obtain volume velocity distribution over a surface, adapted for a given radiation problem. The capacity of the RM method to recreate far-field source radiation has been shown in previous works [11, 20, 21, 22, 19]. Here we propose to use the provided velocity distribution over the surface as an indication of the optimal number and positions of the loudspeakers, as well as their sizes. A brief presentation of the method is given in Sec 2, the description of the problem and numerical simulations are presented in Sec 3 and validated by measurements in Sec. 4. Results are summarized in Sec. 5.

2 THEORY

2.1 Radiation mode method

The "radiation modes" method is inspired by an inverse acoustic imaging technique: the IBEM-NAH regularized by singular value decomposition (SVD) [10] that has been proposed by Veronesi and Maynard [27]. As the derivation of the method has already been described in [21], only a brief summary will be given here.

The pressure radiated by a vibrating object of surface S can be calculated from the following integral formulation [6, 16]:

$$p(\vec{x}) = \int_S \left(\frac{\partial G}{\partial n}(\vec{x}-\vec{x}_s) \;\; p_s - G(\vec{x}-\vec{x}_s) \frac{\partial p_s}{\partial n} \right) dS \tag{1}$$

where $\vec{x}$ is the location of a point anywhere outside S, $\vec{x}_s$ is the location of an element dS of S, $p_s = p(\vec{x}_s)$ is the parietal pressure at $\vec{x}_s$, ∂n denotes the normal derivative on dS and G is the usual Green function $G(\vec{x}-\vec{x}_s) = \frac{1}{4\pi} \frac{e^{jk|\vec{x}-\vec{x}_s|}}{|\vec{x}-\vec{x}_s|}$, assuming a $e^{-j\omega t}$ time convention.

Formulation 1 may be extended over the surface S, thus relating the surface pressure p_s to the normal component of the vibration pattern $\frac{\partial p_s}{\partial n}$ over S. This integral equation can then be solved numerically by discretizing the source surface S with an adequate mesh. Assuming that the pressures and velocities are constant over each mesh element, the formulation 1 may be reduced to the following matrix form [14, 28]:

$$\frac{1}{2}\mathbf{p_s} = \mathbf{M}\mathbf{q_s} - \mathbf{D}\mathbf{p_s} \tag{2}$$

where $\mathbf{q_s}$ is the discretization of the normal component of the vibration pattern over S. A pressure $\mathbf{p_s}$ over S can then be expressed as $\mathbf{p_s} = \mathbf{Z}\mathbf{q_s}$, where the impedance matrix $\mathbf{Z}$ is computed as:

$$\mathbf{Z} = \left[\frac{1}{2}\mathbf{I} + \mathbf{D} \right]^{-1} \mathbf{M} \tag{3}$$

where $\mathbf{I}$ is the identity matrix.

The impedance matrix $\mathbf{Z}$ defined by eq. 3, which is independent of any actual vibration pattern, may then be expanded trough a SVD. The resulting singular vectors are independent solutions of the associated radiation problem, called the radiation modes (RMs). The present approach assumes that the target pressure zone is in the far-field, where only the propagative terms are significant. The imaginary part of the impedance matrix, corresponding to the evanescent field, can thus be neglected and the RMs can therefore be calculated by SVD of the real part only of the impedance matrix:

$$\Re(\mathbf{Z}) = \mathbf{U}\Sigma\mathbf{V}^* \tag{4}$$

where $*$ means the conjugate transpose of a matrix. $\mathbf{U}$ and $\mathbf{V}$ are sets of vectors corresponding to the pressure and the volume velocity of each "mode" respectively, and Σ is a diagonal matrix composed of positive real values related to the radiation efficiencies of the RMs.

2.2 Expansion coefficients

The far-field pressure anywhere around the source $\mathbf{p_t}$ can therefore be expressed as the superposition of N RMs: $\mathbf{p_t} = \mathbf{H_t}\mathbf{w}$ where $\mathbf{H_t}$ is the transfer matrix relating RMs over S to the corresponding pressures $\mathbf{p_t}$ at the target locations. The weight coefficients $\mathbf{w}$ determine the excitation of each term of the series. Using the Moore-Penrose pseudoinverse of transfer matrix $\mathbf{H_t}$ between modes and pressures $\mathbf{p_t}$, the coefficients $\mathbf{w}$ can be determined as:

$$\mathbf{w} = \frac{\mathbf{H_t^*}}{\| \mathbf{H_t} \|^2} \mathbf{p_t} \tag{5}$$

A simple regularization method consists in truncating the expansion to the N most efficient RMs, where N is chosen according to the desired accuracy (*eg* by keeping, say, 98% of the cumulated efficiency in matrix Σ). Equation 5 is thus restricted to rank N when computing $\mathbf{w}$.

This allows to estimate a volume velocity $\mathbf{q}$ distribution over the surface S, which radiates a desired pressure $\mathbf{p_t}$, with maximum efficiency. Here $\mathbf{q}$ is simply obtained as the superposition of the RM volume velocities $\mathbf{V}$ weighted by the coefficients $\mathbf{w}$ (eq. 6), and it will be used to identify optimal positions of discrete sources for pressure synthesis.

$$\mathbf{q} = \mathbf{V}\mathbf{w} \tag{6}$$

2.3 Sound zone as a pressure target

We now consider two zones: one with high acoustic energy ("bright zone" with pressure $\mathbf{p_B}$) and the other with lower pressure level ("dark zone" with pressure $\mathbf{p_D}$). In the present study, the target pressure $\mathbf{p_t}$ is defined over the bright zone, and only a mean pressure level D_0 is defined in the dark zone. Therefore, we need to relax the constraints expressed at all points by equation 5 when computing $\mathbf{w}$. It is here proposed to use a classical acoustic contrast control (ACC) technique. We chose the pressure matching method [5] which objective is to impose a target pressure with maximum level in the bright zone, while creating an acoustic contrast between the bright and the dark zones, by minimizing of the following cost function J:

$$J = [\mathbf{p_B} - \mathbf{p_t}]^*[\mathbf{p_B} - \mathbf{p_t}] + [\mathbf{p_D^*}\mathbf{p_D} - D_0] \tag{7}$$

The optimal source strength $\mathbf{q_{opt}}$, that minimizes the cost function J is:

$$\mathbf{q_{opt}} = [\mathbf{G_B^*}\mathbf{G_B} + \mu\mathbf{G_D^*}\mathbf{G_D}]^{-1}[\mathbf{G_B^*}\mathbf{p_t}] \tag{8}$$

here μ is a positive real coefficient which tunes the relative importance of the contrast condition, $\mathbf{G_B}$ and $\mathbf{G_D}$ are the transfer matrices relating source strengths with pressures at M_B or M_D points, respectively located in bright and dark zones.

This technique can be incorporated into the RM method, according to the similarities between pressure representation through the source strength in ACC techniques and the one through the RMs:

$$\mathbf{p} = \mathbf{G}\mathbf{q} = \mathbf{H}\mathbf{w} \tag{9}$$

Here, $\mathbf{G}$ is the transfer matrix relating N loudspeakers membrane volume velocities $\mathbf{q}$ with pressures $\mathbf{p}$ in M points, and $\mathbf{H}$ is the transfer matrix between N surface RMs and pressures $\mathbf{p}$ in M points. Hence, instead of driving array sources by the adapted signals $\mathbf{q_{opt}}$ from eq. 8, one can "drive" the series of modes using adapted RM coefficients $\mathbf{w_{opt}}$ determined as:

$$\mathbf{w_{opt}} = [\mathbf{H_B^*}\mathbf{H_B} + \mu\mathbf{H_D^*}\mathbf{H_D}]^{-1}[\mathbf{H_B^*}\mathbf{p_t}] \tag{10}$$

Eq. 6 is thus rewritten as:

$$\mathbf{q} = \mathbf{V}\mathbf{w_{opt}} \tag{11}$$

3 SIMULATIONS

3.1 Test case

As a first case study, we use a $53 \times 53 \times 18$ cm enclosure placed at 70 cm in front of a rigid wall. Acoustically bright zone is a 40×40 cm square spot on the wall in front of enclosure. The target pressure level is 100 dB. A 1 m diameter zone around bright zone and 1 m diameter cylinder around enclosure ended by an half-sphere compose the dark zone, in which the pressure level should be attenuated by at least 15 dB. The problem is depicted in Figure 1.

For the numerical calculation, the enclosure surface is discretized by a mesh with 3 mm elements, bright zone by $M_B = 81$ points regularly spaced by 5 cm, and dark zones on the wall (D1) and around the surface (D2)

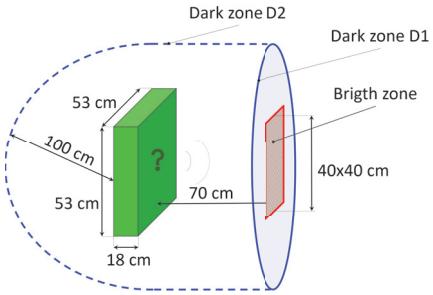

Figure 1. Problem schema

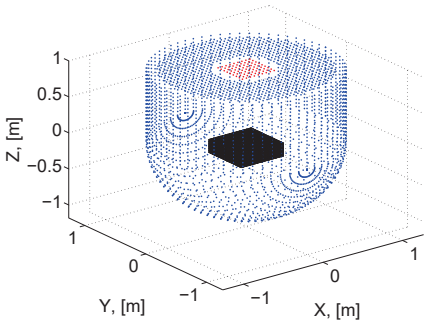

Figure 2. Numerical representation of the problem

are presented by $M_{D1} = 864$ and $M_{D2} = 2324$ points respectively (Figure 2). The rigid wall is modelled as an infinite reflecting plane.

The RMs and their corresponding $\mathbf{H_B}$ + $\mathbf{H_D}$ matrices were computed using a custom BEM code developed at LMA, dedicated to field expansion ("FELIN": Field ELement INdependence).

3.2 Modal volume velocity interpretation

For now, analysis of the modal velocity distribution is a tricky task for two main reasons. First, a trade-off must be found to determine the number N of RMs, as it must allow an accurate enough description without leading to complex vibrating shapes which could hardly be reproduced in practice. A second challenge is to convert the frequency-dependant velocity distributions over surface S into a small set of frequency-independent discrete sources.

First simulations showed that up to 1 kHz, 20 to 35 modes can be sufficient for sound reconstruction. Thus, we took 35 modes to estimate the distributions of the modal volume velocity over S. They are presented in Figure 3 at several frequencies (200 Hz, 500 Hz, 750 Hz and 900 Hz). Visual analysis helped to establish the general features of the velocity distributions. Almost for all frequencies there are 5 accentuated zones at the rear side of the structure: 4 zones in-phase at the corners and the 1 in the center. The locations for the front side is less obvious: At most frequencies it does not seem to play any important role in the generation of sound. Though, at medium frequencies its contribution becomes very significant, with a vibrating central zone of size varying with frequency.

After few tests that are detailed in [18], a 4 channels system has been defined: (1) 1 loudspeaker in the front side center (*Audax HM 170 GO* with membrane diameter of 13 cm), (2) 16 small diameter loudspeakers building an annular zone around the center (*Aura NSW2-326-8A* with membrane diameter of 4,4 cm), (3) 1 loudspeaker on the rear side center *Beyma 5P200/Fe*, membrane diameter of 12 cm, (4) 4 loudspeakers at the rear side corners *Dayton RS100-8*, membrane diameter of 7.7 cm. On the front side, the combination of the center loudspeaker with the ring of smaller ones allows to vary the size of the vibrating zone. This source arrangement is inspired by a previous work where a loudspeaker ring was used to obtain a wide reproduction zone [12].

After selecting the transducer locations over the enclosure, the driving signals may be computed by one of the sound zone techniques as for a conventional array. In the present work we use again the pressure matching technique. The optimal source strength vector $\mathbf{q_{opt}}$ is thus obtained from equation 8.

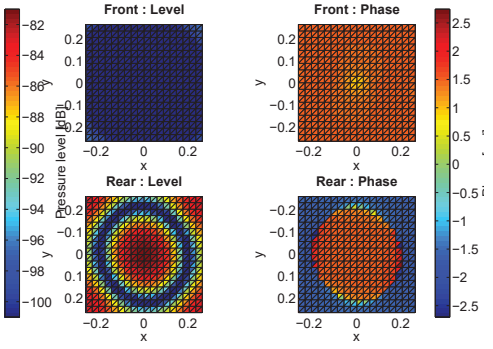

(a) 200 Hz

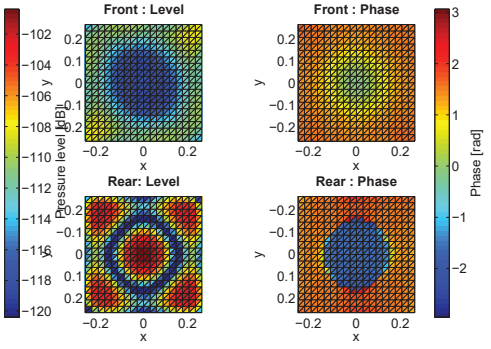

(b) 500 Hz

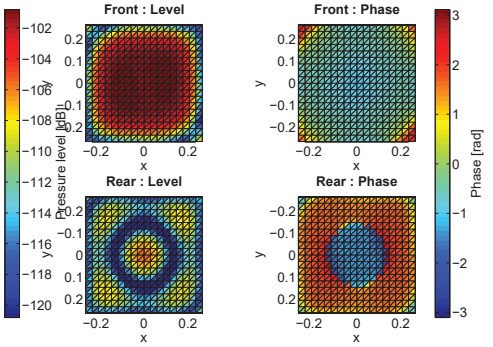

(c) 750 Hz

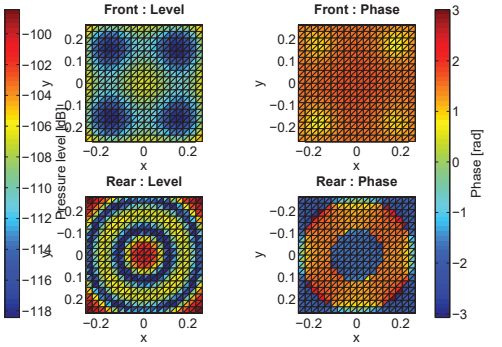

(d) 900 Hz

Figure 3. Modal volume velocity distribution over the surface for different frequencies (level and phase, front and rear view)

3.3 Design validation

To control the performance of the system, we propose to use 3 metrics. Global acoustical contrast C_G, describes the difference of the acoustical power in the bright and dark zones. Higher value of this metric indicates better performance. Expressed in decibels, the global contrast is [9]:

$$C_G = 10\log_{10}\left(\frac{M_D}{M_B} \times \frac{\mathbf{p_B}^* \mathbf{p_B}}{\mathbf{p_D}^* \mathbf{p_D}}\right) \tag{12}$$

Similarly, the local acoustical contrast C_L is defined between the pressure over the bright zone zone, and the one over the dark zone D_1, both in front of the system.

$$C_L = 10\log_{10}\left(\frac{M_{D1}}{M_B} \times \frac{\mathbf{p_B}^* \mathbf{p_B}}{\mathbf{p_{D1}}^* \mathbf{p_{D1}}}\right) \tag{13}$$

The normalised reproduction error compares the desired $\mathbf{p_t}$ and reproduced $\mathbf{p_B}$ fields in the bright zone [7]:

$$E_R = 10\log_{10}\left(\frac{(\mathbf{p_t} - \mathbf{p_B})^* (\mathbf{p_t} - \mathbf{p_B})}{\mathbf{p_B}^* \mathbf{p_B}}\right) \tag{14}$$

For this last metric, a smaller value indicates a better performance, with 0 dB corresponding to a high error level (equal to the target field level).

Figure 4 presents the simulation of the 4-channel source metrics while Figure 5 shows the pressure field radiated at M_B and M_D points for several frequencies. We can observe the ability of proposed source to maintain an almost constant contrast level between the zones at all frequencies as well as good synthesis accuracy.

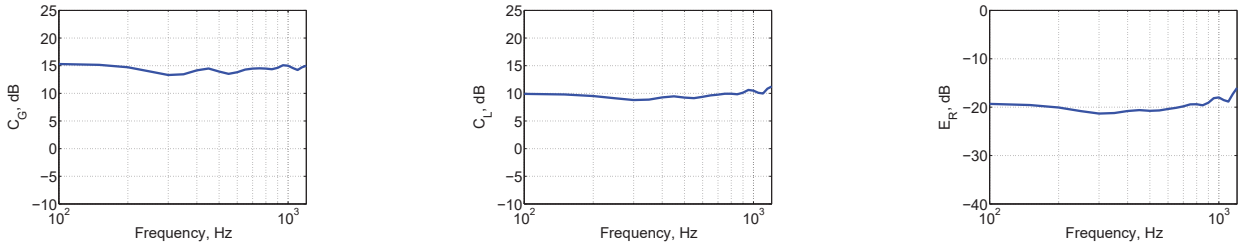

(a) Global contrast (b) Local contrast (c) Reproduction error

Figure 4. Metrics for the numerical model

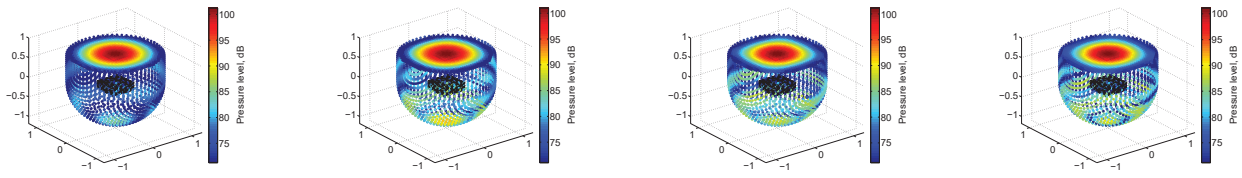

(a) 200 Hz (b) 500 Hz (c) 750 Hz (d) 900 Hz

Figure 5. Radiated pressure maps of the numerical model

4 REALISATION AND MEASUREMENT

An experimental validation was held in the CTTM semi-anechoic chamber. The system was fixed on a turning table flush mounted in the room floor. The pressure behind the system was measured thanks to a wooden support equipped with 18 microphones (Figures 6 and 7). Assuming symmetrical radiation of sources, measurements of the $\frac{1}{4}$ of space were taken, by rotating the system 90° around its axis. Pressure measurements (zones B and $D1$) were also recorded on the floor by using a metallic stem holding 11 microphones spaced by 10 cm (Figure 8).

The driving signals were generated by a RME Fireface US audio interface and amplified for different groups of loudspeakers by a multichannel amplifier HPA QA4150. Pressure field was measured with 29 $\frac{1}{4}$" PCB 130D21 microphones and acquired through National Instruments boards NI PXI-1045 using the INTAC software.

The driving commands were computed from eq. 8, using measured transfer functions between 4 channels and microphones. Satisfactory results are presented in Figures 9 and 10, showing a constant contrast level and accurate target pressure synthesis. A discrepancy between desired and real pressure generation in the bright zone can however be noticed at 200 Hz. It is probably due to the differences between the 4 actual corner loudspeakers, assumed identical and identified as a single source during the computation of the commands.

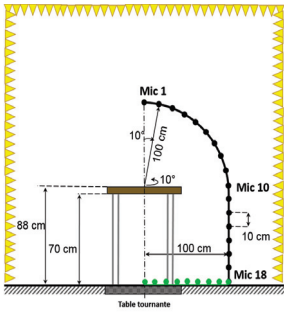

Figure 6. Schema of the measurement setup

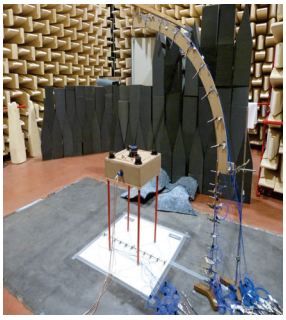

Figure 7. Photo of the measurements setup

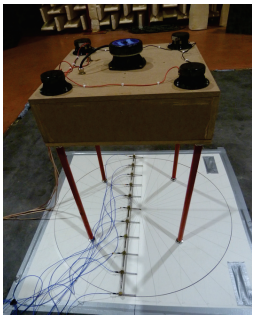

Figure 8. Photo of the source on the turning table

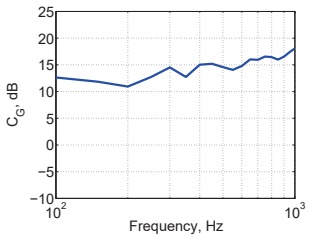

(a) Global contrast

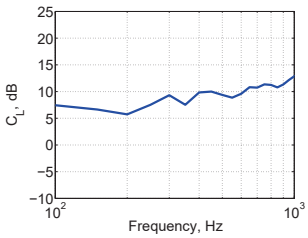

(b) Local contrast

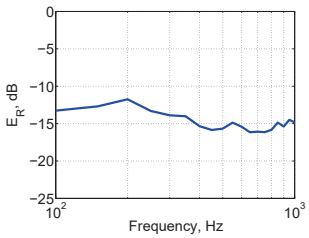

(c) reproduction error

Figure 9. Metrics for the experimental mock-up

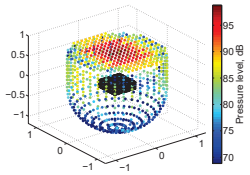

(a) 200 Hz

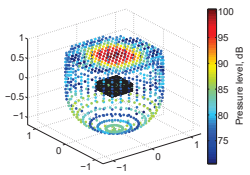

(b) 500 Hz

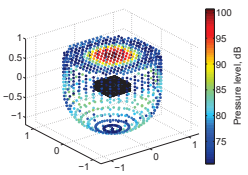

(c) 750 Hz

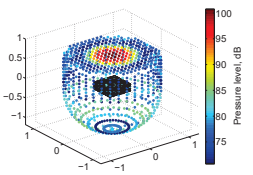

(d) 900 Hz

Figure 10. Measured maps of the radiated field for several frequencies

5 CONCLUSION

The aim of the present work consisted in designing a directive source able to generate a predefined field with a high spatial contrast. In order to reduce the number of loudspeakers to the minimum possible, we used the radiation mode method as an indication of the most suitable transducer locations and sizes. The visual analysis has permitted to design a source, that responds to all imposed conditions. First numerical and experimental results are very promising, and motivate further investigations. For instance, genetic algorithms could be used to select the optimal number, diameters and locations of speakers on the enclosure using the RMS.

ACKNOWLEDGEMENTS

Authors would like to thank Marie-Hélène Moulet for conducting the measurements and the CTTM design engineering department for the source production.

REFERENCES

[1] F. Asano, Y. Suzuki, T. Sone, and D. Swanson. Optimization of control source location in active control systems. In *Proceedings of Active 95*, pages 489–498, 1995.

[2] F. Avanzini, A. Belussi, A. Dal Palù, A. Dovier, and D. Rocchesso. Optimal placement of acoustic sources in a built-up area using CLP (FD). In *APPIA-GULP-PRODE 2002, Joint Conf. on Declarative Programming*, pages 139–154, 2002.

[3] K. Baek. Natural algorithms for choosing source locations in active control systems. *Journal of Sound and Vibration*, 186(2):245–267, 1995.

[4] E. Benzaria and V. Martin. Constrained optimization of secondary source locations: multipolar arrangements. In *Proceedings of Active 95*, pages 499–510, 1995.

[5] T. Betlehem, W. Zhang, M. A. Poletti, and T. D. Abhayapala. Personal sound zones: Delivering interface-free audio to multiple listeners. *IEEE Signal Processing Magazine*, 32(2):81–91, 2015.

[6] M. Bruneau. *Fundamentals of acoustics*. CA: ISTE Ltd, 2006.

[7] J. Chang and F. Jacobsen. Sound field control with a circular double-layer array of loudspeakers. *The Journal of the Acoustical Society of America*, 131(6), 2012.

[8] G. N. Charalampopoulos, S. T. Mouzakitis, and C. G. Provatidis. Gradient optimisation methods for the positioning of active noise control actuators in enclosures. *International Journal of Acoustics and Vibrations*, 9(4):163–174, 2004.

[9] J.-W. Choi and Y.-H. Kim. Generation of an acoustically bright zone with an illuminated region using multiple sources. *The Journal of the Acoustical Society of America*, 111(4):1695–1700, 2002.

[10] G. H. Golub and C. F. V. Loan. *Matrix Computations*, volume 10. Physics Today, 1996.

[11] P. Herzog, R. Guillermin, P. Lorin, and V. Chritin. Identification of a vibration pattern from pressure measurements and radiation modes. In *EuroNoise*, Maastricht, Netherlands, 2015.

[12] P. Herzog and M. Melon. An active cell to improve transmission loss of partition walls at lower frequencies. In *Euronoise*, Prague, Czech Republic, 10-13 June 2012.

[13] J. K. Kim and J.-G. Ih. On the positioning of control sources for active noise control in 3-dimensional enclosed space. In *Proceedings of Active 95*, pages 510–518, 1995.

[14] S. Kirkup. *The Boundary Element Method in Acoustics*. Integrated Sound Software, 1998.

[15] D. A. Manolas, T. Gialamas, and D. T. Tsahalis. A genetic algorithm for the simultaneous optimization of the sensor and actuator positions for an active noise and/or vibration control system. In *Proceedings of Internoise 96*, pages 1187–1192, Liverpool, UK, 30 July - 2 August 1996.

[16] P. M. Morse and K. U. Ingard. *Theoretical acoustics*. Princeton University Press, 1968.

[17] S. Pottie and D. Botteldooren. Optimal placement of secondary sources for active noise control using a genetic algorithm. In *Proceedings of Internoise 96*, pages 1101–1104, Liverpool, UK, 30 July - 2 August 1996.

[18] M. Sanalatii. *Synthèse d'un champ acoustique avec contraste spatial élevé*. PhD thesis, Le Mans University, 2018.

[19] M. Sanalatii, P. Herzog, R. Guillermin, M. Melon, N. Poulain, and J.-C. Le Roux. Estimation of loudspeaker frequency Response and directivity using the radiation-mode method. *J. Audio Eng. Soc.*, 67(3):101–115, 2019.

[20] M. Sanalatii, P. Herzog, M. Melon, R. Guillermin, J.-C. Le Roux, and N. Poulain. Identification du profil vibratoire d'un haut-parleur monté sur une enceinte close a partir de mesures de pression acoustique en champ proche. In *Congrès Français d'Acoustique*, number 215, Le Mans, France, 2016.

[21] M. Sanalatii, P. Herzog, M. Melon, R. Guillermin, J.-C. Le Roux, and N. Poulain. Measurement of the frequency and angular responses of loudspeaker systems using radiation modes. In *the 141th Audion Engineering Society Convention*, number preprint 9615, Los Angeles, USA, 2016 September 29th - October 1st.

[22] M. Sanalatii, L. Vindarola, C. Vasseur, P. Herzog, M. Melon, R. Guillermin, N. Poulain, and J.-C. Le Roux. Assessment of the radiation mode method for *in situ* measurements of loudspeaker systems. In *the 142nd Audion Engineering Society Convention*, number preprint 9615, Berlin, Germany, 2017 May 20-23.

[23] A. Sarkissian. Acoustic radiation from finite structures. *The Journal of the Acoustical Society of America*, 90(1):574–578, 1991.

[24] P. Sergent and D. Duhamel. Optimal placement of sources and sensors with minimax criterion for active contriol of a one-dimentional sound field. *Journal of Sound and Vibration*, 207(4):537–566, 1997.

[25] M. Shin, S. Q. Lee, F. M. Fazi, P. A. Nelson, D. Kim, S. Wang, K. H. Park, and J. Seo. Maximization of acoustic energy difference between two spaces. *The Journal of the Acoustical Society of America*, 128(1):121–131, 2010.

[26] M. F. Simón Gálvez, S. J. Elliott, and J. Cheer. A superdirective array of phase shift sources. *The Journal of the Acoustical Society of America*, 132(2):746–756, 2012.

[27] W. Veronesi and J. Maynard. Digital holographic reconstruction of sources with arbitrary shaped surfaces. *Journal of the Acoustical Society of America*, 85(2):588–598, 1989.

[28] S. F. Wu. *The Helmholtz Equation Least Squares Method*. Springer, 2015.